

Supporting Information

Facile synthesis of a glutathione-depleting Cu(II)-half-salamo- based coordination polymer for enhanced chemodynamic therapy

Wenting Guo*, Tongxi Ji, Yunhu Deng, Jia Liu, Yantong Gou, Wenkui Dong

School of Chemistry and Chemical Engineering, Lanzhou Jiaotong University, Lanzhou, Gansu 730070, China

* Corresponding author. E-mail: guowenting@mail.lzjtu.cn. Fax: (+86) 931-4938703 (Dr. Wenting Guo).

General Information

Instrument description: X-ray powder diffraction (XRD) patterns of the nanomaterials were recorded on a Bruker AXS D8-Advanced diffractometer with Cu K α radiation ($\lambda=1.5418\text{\AA}$). X-ray photoelectron spectroscopy (XPS) measurements were performed on a PHI-5702 multifunctional spectrometer using AlK α radiation. IR spectra were recorded in the range of 4000-400 cm^{-1} using a Vertex70 FT-IR spectrophotometer via KBr pelletization technique. Fluorescence and UV-vis measurements were done using F-7000 FL spectrophotometer and U-3900H spectrophotometer at room temperature, respectively. High resolution Mass spectrometry were recorded using a LTQ-Obitrap-ETD instrument. Phosphate Buffered Saline (PBS) and Dulbecco's modified Eagle's medium (DMEM) were obtained from GE Healthcare Life Sciences HyClone Laboratories (Logan, UT, USA). Fetal bovine serum (FBS) and Trypsin-EDTA were bought from Gibco (USA). Glutathione (reduced) was from Solarbio. Cell counting kit-8(CCK-8) was bought from Dojindo (Japan).

Materials: Hydrogen peroxide (H_2O_2 , 30%) and sodium hydroxide (NaOH), Hydrochloric acid (HCl) were from Kelon Chemical Reagent Factory. Methylene Blue (MB) was purchased from Aladdin. 5-bromo-2-hydroxybenzaldehyde, 3-hydroxy-2-naphthoic acid, fluorescein and terephthalic acid (TPA) were from Energy Chemical. Copper acetate monohydrate ($\text{Cu}(\text{OAc})_2\cdot\text{H}_2\text{O}$) were from Macklin. *N,N*-Dimethylformamide (DMF), ethanol, trichloromethane, ethyl acetate and dimethyl sulfoxide (DMSO) were from Rianlon. All of the chemicals were used without further purification except as noted. Distilled water was used in all the experiment.

Cell Culture and Cell Viability: Mouse embryonic fibroblast (NIH-3T3) cells and human cervical cancer (Hela) cell were cultured under their respective conditions. The cytotoxicity was tested by a cell counting kit-8 (CCK-8 kit). Hela cells and NIH-3T3 cells were cultured on 96-well plates at 5×10^3 cells/well. After 12 h, the cells were incubated with 20 $\mu\text{g}/\text{mL}$ of CuCP, and then the cells were irradiated for 2 min (808 nm, 0.5 W/cm^2) or without any treatment. The cell viability was determined by measuring the absorbance of CCK reagent at 450 nm after 24 h with a microplate reader (318c-microplate reader).

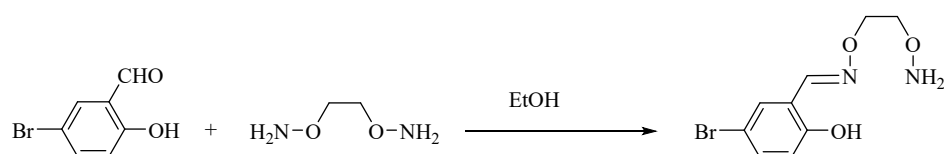


Figure S1. Synthetic route of HL¹.



Figure S2. The digital picture of the mass production of CuCP.

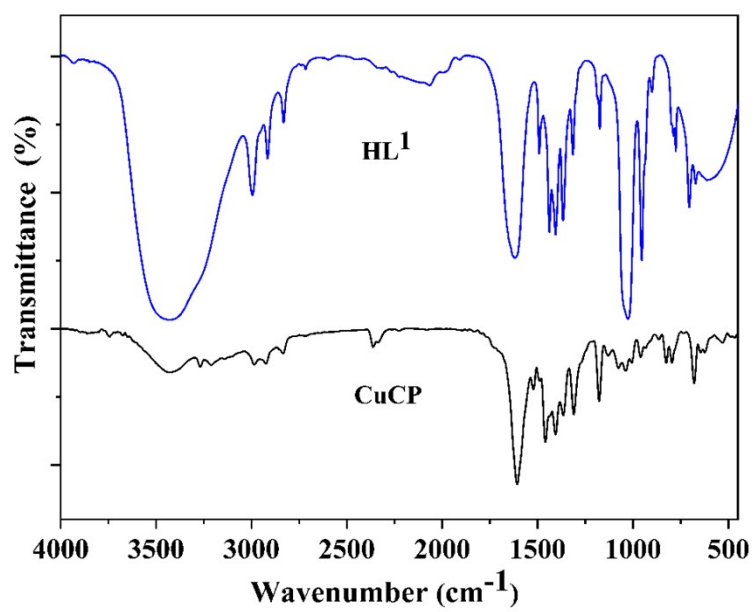


Figure S3. IR absorption spectra of HL¹ and the CuCP.

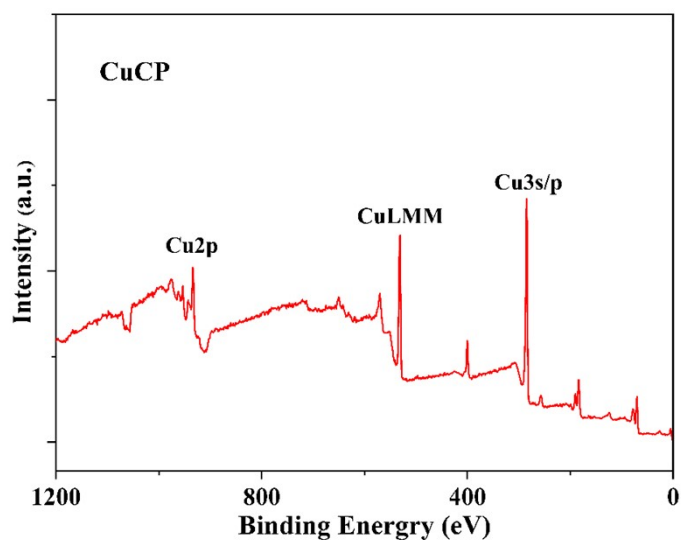


Figure S4. XPS spectra of the CuCP.

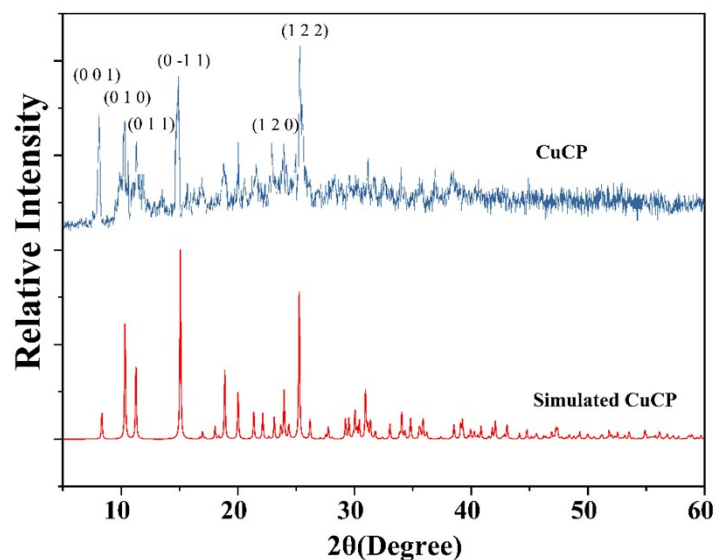


Figure S5. XRD patterns measured and simulated for CuCP.

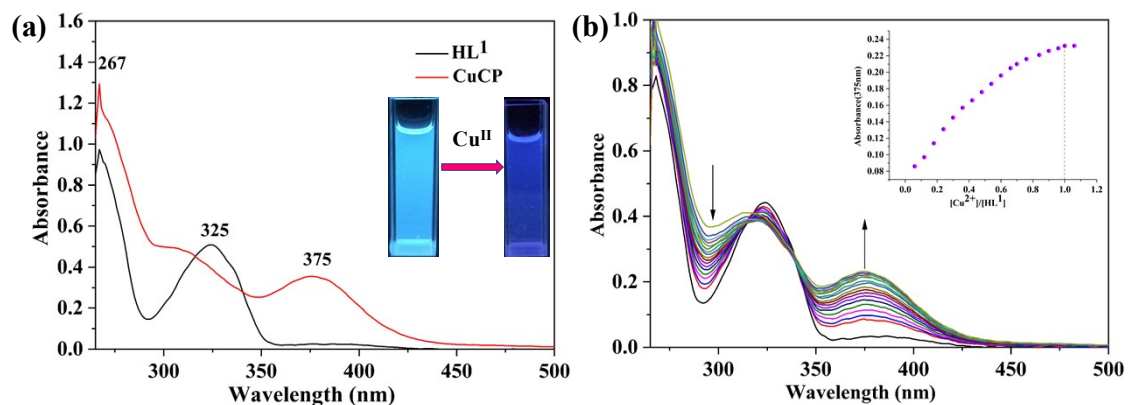


Figure S6. (a) The UV-Vis spectra of HL¹ and polymer-Cu dissolved in dimethylformamide/H₂O solvent; (b) UV-vis spectral changes of HL¹ upon addition of Cu(II) ions. The inset shows the plot of absorbance at 375 nm against the molar ratio of [Cu²⁺]/[HL¹].

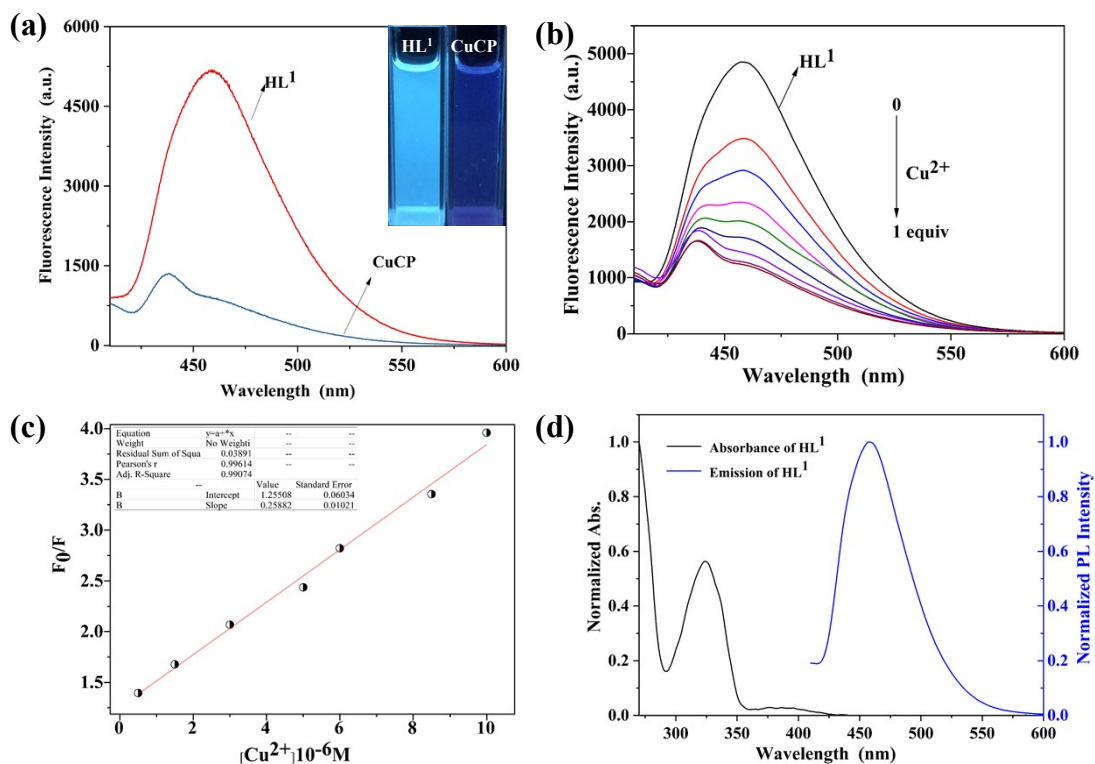


Figure S7. (a) Fluorescent spectra of HL¹ and CuCP dissolved in mixed solvent (5.0 × 10⁻⁵ M, dimethylformamide: H₂O = 9:1) upon excitation at 385 nm; (b) Fluorescent spectrum variations of HL¹ solution (c = 1 × 10⁻⁵ M) upon increase of various amounts of Cu(II) ions (0–1.0 equiv) in dilute dimethylformamide solutions at room temperature; (c) The linear relation between the additions of Cu(II) and fluorescent intensity. (d) Excitation and emission spectra of CuCP reacted with GSH.

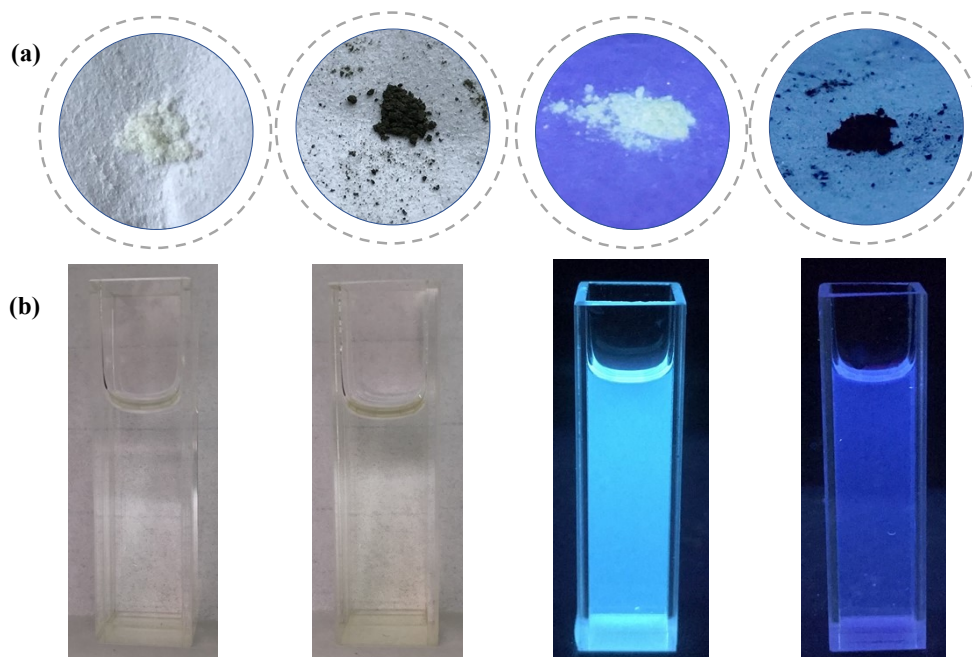


Figure S8 (a) comparison of solid HL¹ and CuCP under natural light and LED UV lamp (365nm). (b) comparison of solutions of HL¹ and CuCP (c = 1 × 10⁻⁵ M) under natural light and LED uv lamp (365nm).

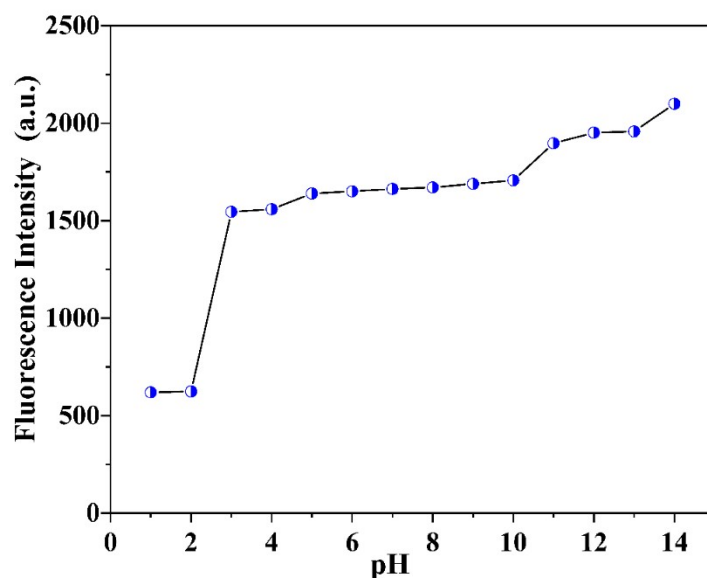


Figure S9. Changes of fluorescence intensity of coordination polymers at different pH values.

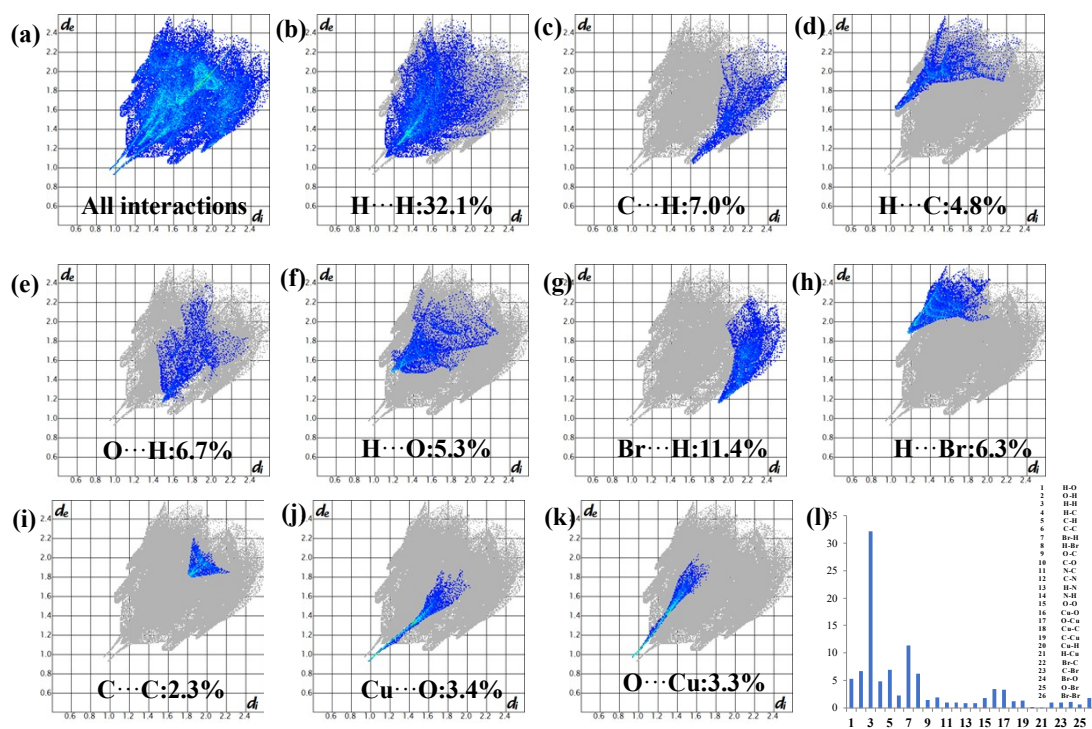


Figure S10. The relative contributions of various intermolecular contacts to the Hirshfeld surface area of the title structure are displayed by the schematic illustration. Fingerprint plots: (a) all contacts involved in the structure; (b) H...H; (c) C...H; (d) H...C; (e) O...H; (f) H...O; (g) Br...H; (h) H...Br; (i) C...C; (j) Cu...O; (k) O...Cu; (l) Comparison of all interactions on the Hirshfeld surface of a CuCP crystal.

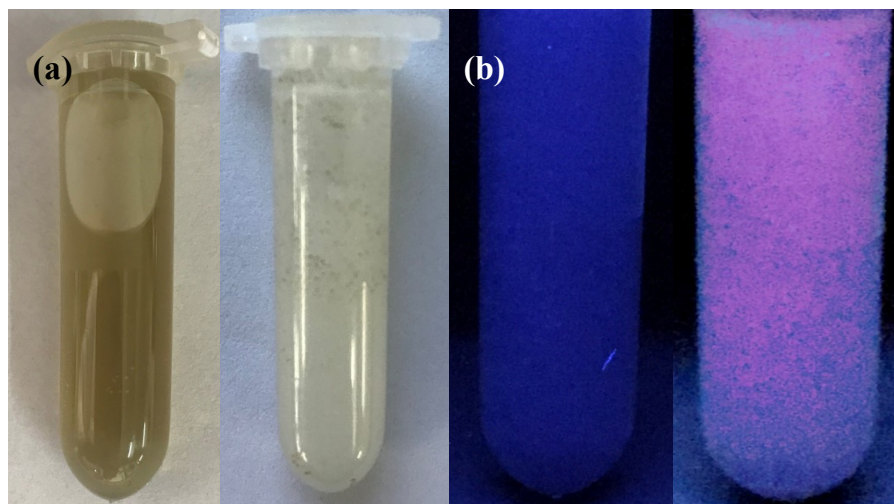


Figure S11. (a) Color change of the **CuCP** before (left) and after (right) reaction with GSH. (b) Digital pictures of **CuCP** before (left) and after (right) reaction with GSH under a UV light ($\lambda_{em}=254$ nm).

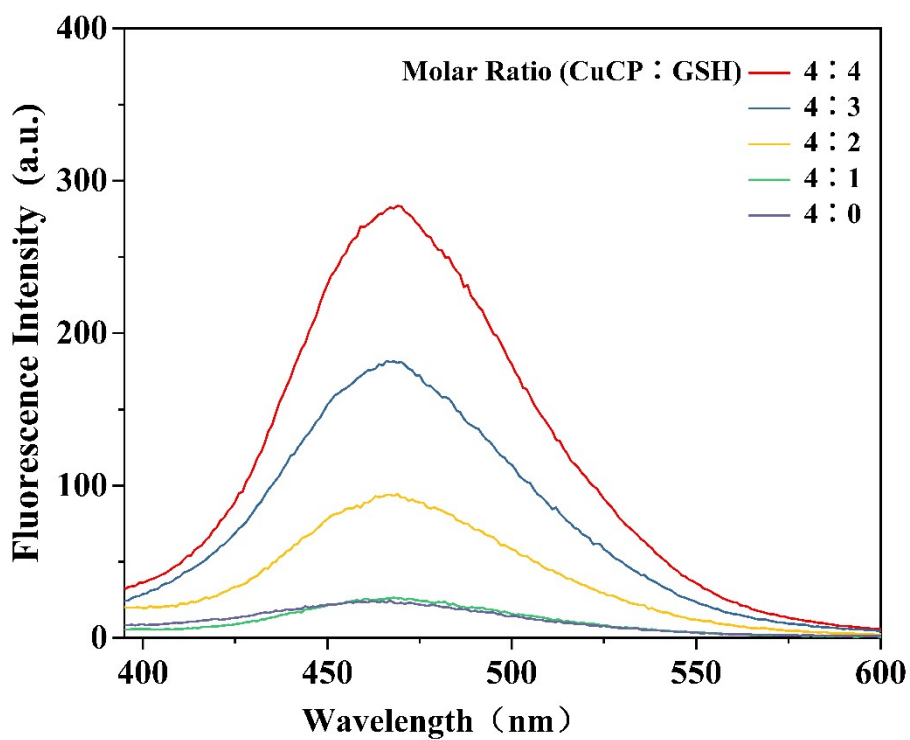


Figure S12. Emission spectra of Cu (II) polymer mixed with GSH at different ratios.

Figure S15. (a) ^1H NMR of the supernatant in D_2O (blue line), commercial GSH (yellow line) and commercial GSSG (red line), supernatant in D_2O . (b) HRMS of the supernatant in D_2O .

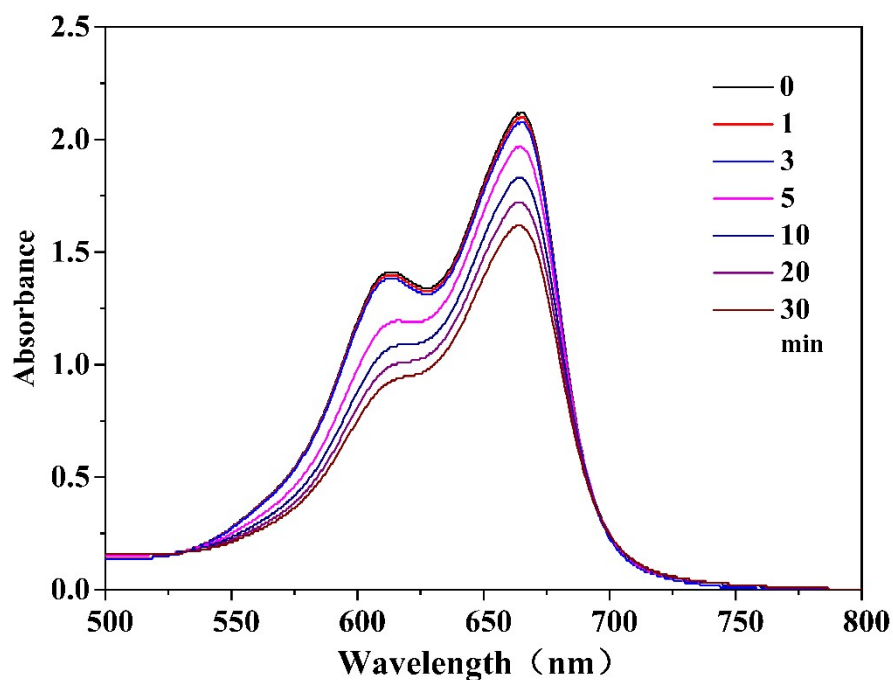


Figure S16. The MB degradation under the CuCP plus H_2O_2 condition.

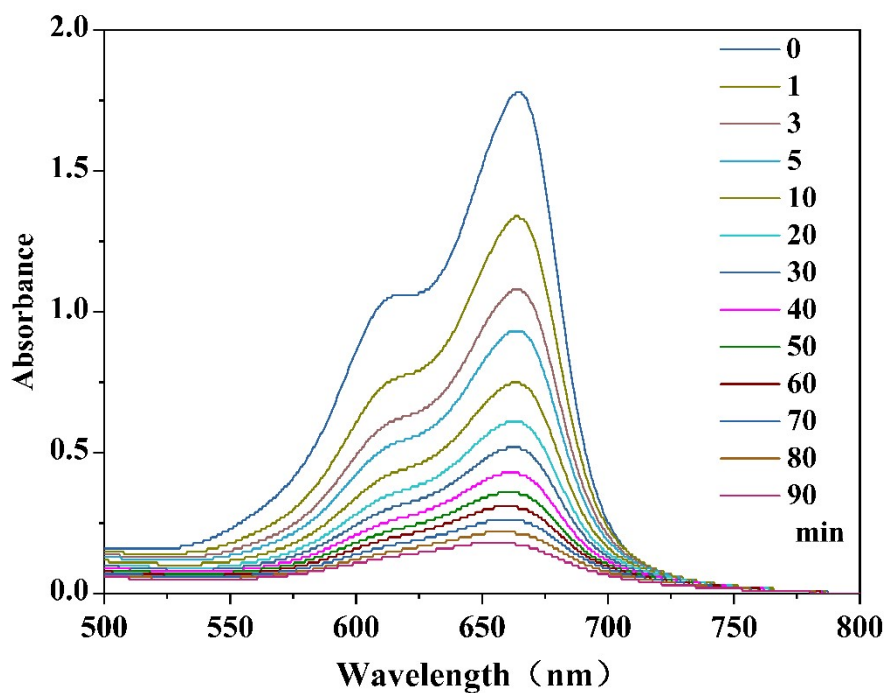


Figure S17. Degradation of MB with time under CuCP-G and H_2O_2 (pH=6.5).

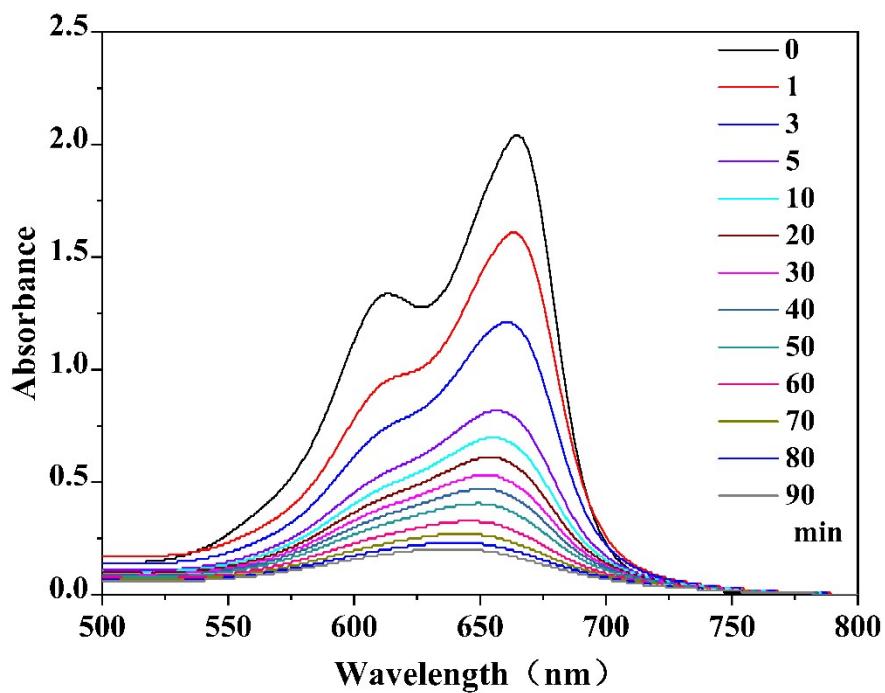


Figure S18. Degradation of MB with time under CuCP-G and H₂O₂ (pH=5.0).

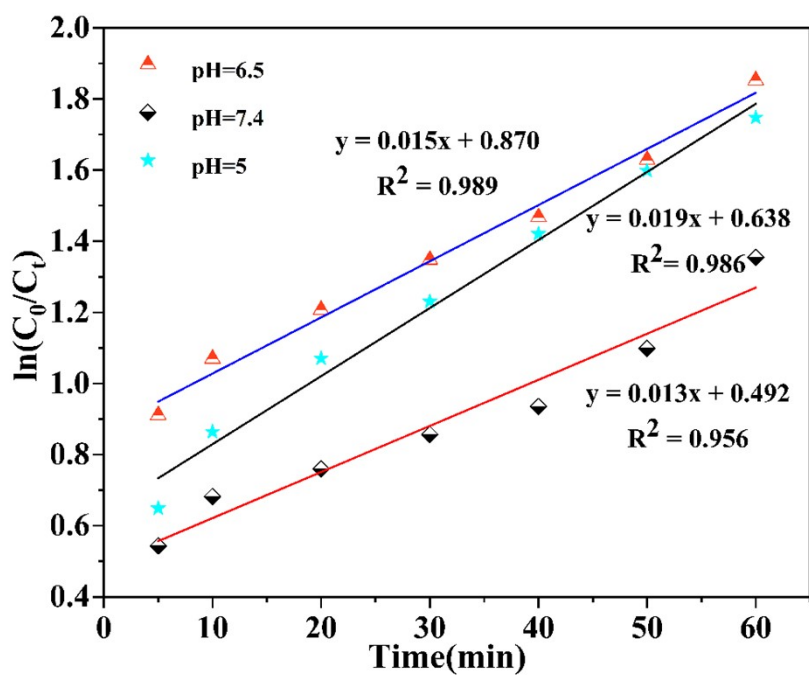


Figure S19. Degradation rates of MB under different pH conditions.

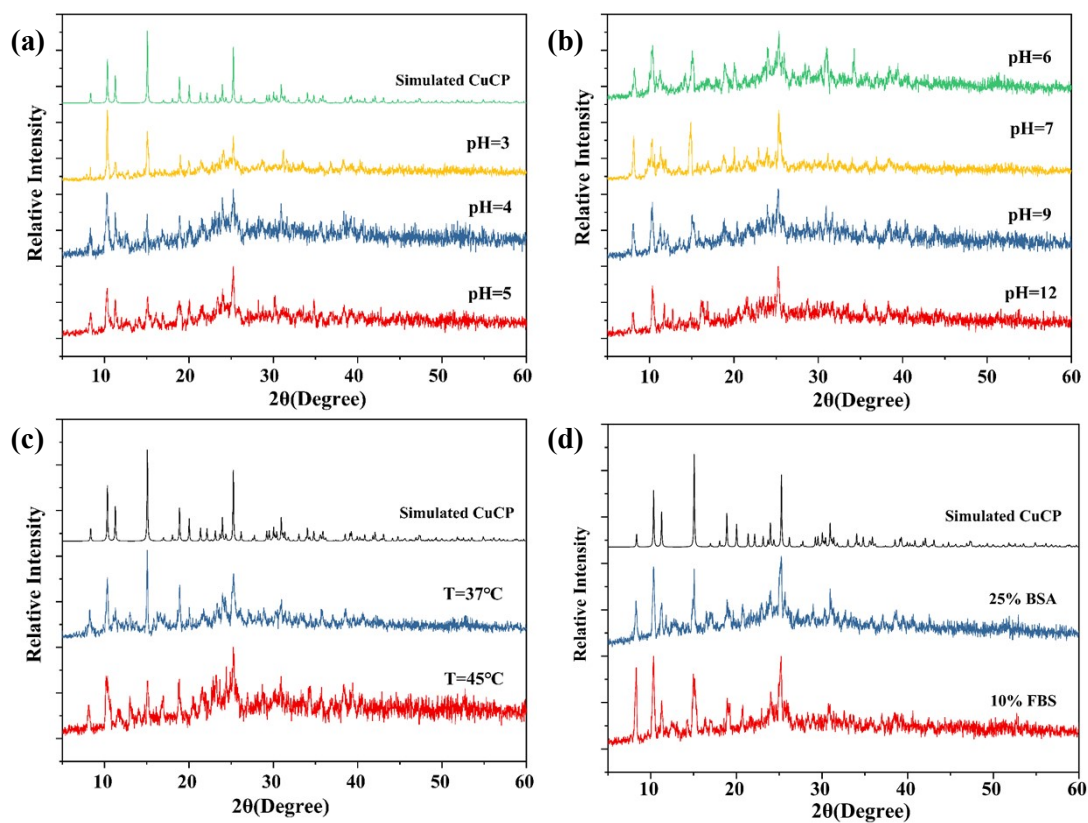


Figure S20. (a) XRD patterns of a 40 mM CuCP solutions under different pH (pH=3, 4, 5) after 12 h. (b) Under different pH (pH=6, 7, 9, 12) after 12 h. (c) Under different temperatures. (d) 10% w/v BSA, and 25% v/v FBS.

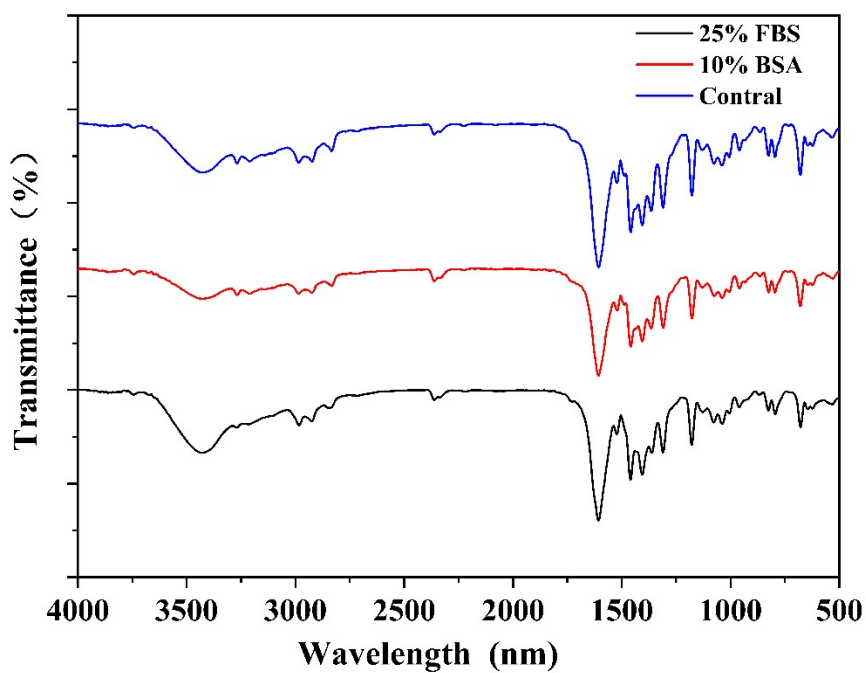


Figure S21. FT-IR spectra of a 40 mM CuCP solutions in media with 10% w/v BSA and 25% v/v FBS.

Table S1. Crystal data and the structure refinements for **CuCP**.

Complex	CuCP
Formula	C ₉ H ₈ BrCuNO ₃
Formula weight	321.61
Temperature (K)	273(2)
Wavelength (Å)	0.71073
Crystal system	Triclinic
Space group	<i>P</i> -1
Unit cell dimensions	
<i>a</i> (Å)	5.3104(2)
<i>b</i> (Å)	9.1877(3)
<i>c</i> (Å)	11.1051(4)
α (°)	72.4130(10)
β (°)	84.1890(10)
γ (°)	76.3400(10)
<i>V</i> (Å ³)	501.63(3)
<i>Z</i>	2
<i>D</i> _c (g cm ⁻³)	2.129
μ (mm ⁻¹)	6.142
<i>F</i> (000)	314
Crystal size (mm)	0.08 × 0.06 × 0.04
θ Range (°)	2.60–28.34
Index ranges	-7 ≤ <i>h</i> ≤ 7, -12 ≤ <i>k</i> ≤ 12, -14 ≤ <i>l</i> ≤ 14
Reflections collected	10184
Independent reflections	2493
R _{int}	0.0844
Completeness	99.4%
Data/restraints/parameters	2493 / 0 / 136
GOF	1.042
Final R ₁ , wR ₂ indices	
[<i>I</i> > 2σ(<i>I</i>)]	0.0306 / 0.0809
R ₁ , wR ₂ indices (all data)	0.0359 / 0.0834
Largest difference peak and hole (e Å ⁻³)	0.777 / -0.801

$$R_1 = \frac{\sum |F_o| - |F_c|}{\sum |F_o|}; wR_2 = \frac{[\sum w(F_o^2 - F_c^2)^2 / \sum w(F_o^2)^2]^{1/2}}{w}; w = [\sigma^2(F_o^2) + (0.0289P)^2 + 31.3296P]^{-1}, \text{ where } P = \frac{(F_o^2 + 2F_c^2)}{3}; \text{ GOF} = \frac{[\sum w(F_o^2 - F_c^2)^2 / (n_{\text{obs}} - n_{\text{param}})]^{1/2}}{w}.$$

Table S2. Selected bond lengths (Å) and angles (°) for **CuCP**.

Bond			
Cu1-O1	1.9023(15)	Cu1-O3	1.9118(15)
Cu1-O3 ^{#1}	1.9230(15)	Cu1-N006	1.9462(19)
Cu1-O1 ^{#2}	2.7298(21)		
Angles			
O1-Cu1-O3 ^{#1}	95.72(6)	O1-Cu1-O3	173.19(7)
O1-Cu1-N006	93.14(7)	O3-Cu1-O3 ^{#1}	77.55(7)
O3 ^{#1} -Cu1-N006	165.99(7)	O3-Cu1-N006	93.67(7)

Symmetric code^{#1}: 2-x, 1-y, 1-z; ^{#2}: 1-x, 1-y, 1-z.

Table S3. Frontier molecular orbital energy (eV) of H₂L² and **CuCP** calculated by B3LYP functional. □ □

	Energy (eV)				
	HOMO-1	HOMO	Energy Gap	LUMO	LUMO+1
H ₂ L ²	-6.9057	-6.2876	4.6876	-1.6000	-0.6082
CuCP	-5.5655	-4.9739	1.7831	-3.1908	-1.6019